

Processing and characterization of PbS nanoparticles by ball milling technique and their applications

Abstract

Lead Sulphide (PbS) nanoparticles were processed using ball milling techniques. The processed PbS nanoparticles were characterized using atomic absorption spectroscopy (AAS), X-ray diffraction (XRD), scanning electron microscopy (SEM), energy dispersive analysis (EDAX), and electrical investigation using four-point probe. The XRD results of the PbS nanoparticles show peaks at the crystal plane (111), (200), (210), (211) and (320). The average size of PbS nanoparticle crystallite is found to be 51.05 nm. The optical energy band gap of PbS nanoparticles dispersed in ethanol was observed to be 3.98 eV and 4.06 eV for PbS nanoparticles dispersed in distilled water. The absorbance of PbS nanoparticles shows that the absorbance values were moderate in the UV region but dramatically decreased as they moved towards the visible and near-infrared regions. The EDX analysis shows that PbS nanoparticles is composed of 54.36% Pb, 36.47% C and 9.16% S. The sheet resistance, resistivity, and conductivity were measured and found to be $1.51 \times 10^7 \Omega/\text{Sq.}$, $3.61 \Omega.\text{cm}$ and $2.77 \times 10^{-1} (\Omega.\text{cm})^{-1}$ for PbS nanoparticles. PbS nanoparticles are classified as promising materials for various electronics and optoelectronic devices based on the determined properties.

Keyword: *Lead sulphide, ball milling technique, X-ray diffraction, surface morphology, electrical*

Introduction

“Lead sulphide (PbS) is an important IV-VI group semiconductor which has a narrow direct band gap of 0.41 eV at room temperature (300 K)” [25]. “Research on PbS nanoparticles are growing on demand because of its exciton Bohr radius which is 18 nm at room temperature. PbS nanoparticles have a high dielectric constant ($\epsilon_0 = 169$ at 300 K) as well as high carrier mobility which leads to them exhibit strong quantum size effect despite of having relatively larger size (greater than 10 nm) along with the large band gap (3.2 eV - 4.4 eV)” [23]. “It is known that nanoparticles which has same order of exciton Bohr radius with larger band gap as comparison to bulk band gap (0.41 eV) is what lead to quantum confinement, the particles may be termed as quantum dot” [13]. PbS nanoparticles finds application in optoelectronics devices such as

light-emitting diodes, photoluminescence, optical switches, IR detectors, solar cell etc due to their unique optical properties.

“In general, nanoparticles are supposed to have nearly half of their atoms contained in top two monolayers which make optical properties highly sensitive to surface morphology”[1]. “In the recent years, nano-sized semiconducting materials have attracted a considerable interest owing to their structural, chemical and physical properties that differs from those of the corresponding bulk materials because of the three-dimensional confinement of electrons and holes in a small volume”. [20]“The number of atoms on the surface is comparable to that inside the particles. Nanoparticles have larger surface-to volume ratio and the atoms on the surface are bound by weaker forces because of missing neighbours that leads to high surface reactivity”. [19]“At the nanoscale, the properties of particles may change in unpredictable ways” [14].

Synthesis of nanomaterials by a low cost, high yield and simple methods had been a great challenge since the very early discovery of nanoscience. Various methods has been explored for the processing and synthesis of nanomaterial. Among the methods, the bottom and top-down approaches have been developed so far for commercial production of nanomaterials. Among the various top-down approaches, high energy ball milling has been widely exploited for the processing and synthesis of various nanomaterials, nanocomposites, nanograins, nanoalloy, and nano-quasicrystalline materials.

“PbS nanoparticles (NPs) has shown strong quantum confinement for relatively large size. Also, their absorption edge can be tuned between red to violet covering the entire visible spectrum”[3][8]. PbS nanoparticles have been prepared using various route but they require sophisticated instruments. Bearing in mind the importance of PbS nanoparticles, development of a simple and economic method of preparation is highly necessary. In this work, lead sulphide ore were reduced to nano size by mechanical milling technique because when reduced to nanoparticles, they possess interesting structural, optical, and electrical properties which cannot be found in their bulk form.

The processed nanoparticles have been characterized using atomic absorption spectroscopy (AAS), X-ray diffraction (XRD), scanning electron microscopy (SEM), energy dispersive analysis (EDAX), and electrical investigation using four-point probe. **2.0 Materials and method**

2.1 Materials used

The materials used for this work are as given as follows: Ball mill, Beakers, Volumetric cylinder, Funnel, Filter paper, Magnetic stirrer, Thermometer, Heating mantle

2.2 Processing of PbS nanoparticles

PbS nanoparticles were processed using the ball milling techniques. The Galena (PbS) ores that was used for this work were collected from Enyigba mining site, Abakaliki, Ebonyi State, Nigeria. The Galena ores were granulated to nano sizes using 5kg laboratory ball mill. The following reagents were used in the preparation of the aqua regia for acid digestion of the samples, Hydrochloric (HCL) and nitric acid (HNO_3), Deionized water.

2.3 Sample preparation for AAS analysis

Procedures

This digestion method used in this work is based on EPA method 3052 and the China National Standard to extract the elements from the soil samples and is not intended for full decomposition of the sample. 2gram of soil samples were weighed directly into 100 mL polypropylene (PP) reaction vessels. Using the same acids combination as the standard for soil samples digestion, 70% HCl and 30% HNO_3 (all concentrated) were added to each sample. Analytical reagent blanks were also prepared and contained only the acids. The vessels were lightly covered with the lids and placed into the block. The samples were digested at 120 °C for 1h. Following the digestion, the cooled digested sample solutions were diluted to final volume of 100.0 mL deionized water and then filtered. The filtrate solution was ready for analysis. The Atomic Absorption Spectroscopy analysis was performed using a Buck Scientific AAS 211.

2.4 Sample preparation for soil electrical conductivity

Procedure

2 gram of the sample was weighed into a beaker and 50 ml of deionized water was added to cover the soil sample complete. The solution was allowed to shake in a mechanical shaker at 15 rpm for 1 hour to dissolve the soil sample. The EC meter was calibrated according to the manufacturer's instructions using the KCl reference solution to obtain the cell constant. The EC was read and recorded accordingly.

2.5 Characterization of PbS nanoparticles

The morphology of the nanoparticles was examined using a scanning electron microscope (SEM). The crystal lattice and peak intensities was investigated using Bruker D8 Advance XRD with Cu-K α radiation ($\lambda = 1.5406 \text{ \AA}$) in the range from 15° to 80° . The elemental composition of a samples was performed using Energy Dispersive X-ray analysis. Buck 210/211ATS compact spectrometer was used in the analysis of the concentration of metallic elements in the given sample based on the amount of energy absorbed. The electrical conductivity of the soil samples was determined using electrical conductivity meter. The optical properties of the nanoparticles were investigated using a Shimadzu UV-1800 visible spectrophotometer in the range of 200 to 1100 nm. The electrical characteristics of nanoparticles was examined using an old Jandel four-point probes (model TY242MP) technique.

3.0 Results and Discussion

3.1 Atomic Absorption Spectroscopy (AAS) Analysis

Table 1 shows the concentration of metallic atom present in PbS nanoparticles. "According to the AAS analysis, the sample of PbS nanoparticles contains 140g/kg of Pb while also including trace amounts of other metals such minor elements like Iron and Copper". [26]

Table 1: AAS analysis of PbS nanoparticles

Elements	PbS Nanoparticles (g/kg)
Lead (Pb)	140.000
Zinc (Zn)	Undetected
Iron (Fe)	0.360
Copper (Cu)	0.003

3.2 Soil electrical conductivity

Table.2 shows the soil electrical conductivity PbS nanoparticles using electrical conductivity metre. The EC analysis shows that PbS nanoparticles has an electrical conductivity value of 103.2 ($\mu\text{S}/\text{cm}$).

Table 2: Soil electrical conductivity PbS nanoparticles

Samples	EC VALUE ($\mu\text{S}/\text{cm}$) @ 28 ^o C
PbS	103.2

3.3 Optical analysis of PbS Nanoparticles

The absorbance result of PbS nanoparticles dispersed in distilled water and ethanol is shown in Figure 1a. When PbS nanoparticles was dispersed in distilled water and ethanol, the absorbance in the UV region of the spectrum was moderate (40%) at wavelengths of 284 nm and 292 nm, before dropping sharply to 1% and 3% respectively. In the visible portion of the spectrum, the PbS nanoparticles dispersed in distilled water showed a slight increase of 2%, which decreased slightly as they proceeded into the NIR region of the spectrum. In the visible spectrum, the ethanol- dispersed PbS nanoparticles showed a shallow pattern that diminished as they proceeded into the NIR range. The PbS nanoparticles exhibited very poor absorption of

radiation in the visible region of the electromagnetic spectrum and moderate absorption in the ultraviolet region.

The transmittance of distilled water dispersed PbS nanoparticles increases from 40% to 98% in the UV-visible region of the spectrum, followed by a shallow fall of 4% in the visible area, which increased slightly as they proceeded into the NIR region of the spectrum while the transmittance of ethanol- dispersed PbS nanoparticles increases from 40% to 94% in the UV-visible region of the spectrum, followed by a shallow increase in the visible and NIR region of the spectrum as seen in Figure 1b. The PbS nanoparticles displayed very high transmittance throughout the UV-VIS-NIR region of the electromagnetic spectrum.

As can be seen in Figure 1c, the distilled water dispersed PbS nanoparticles likewise displayed poor reflection of light which decrease from 20% to 1% in the UV region of the spectrum, followed by a sharp increase of 2% in the visible region which decrease slightly as they proceeded into the NIR region while the reflectance of ethanol- dispersed PbS nanoparticles increases from 20% to 2% in the UV-visible region of the spectrum, followed by a shallow decrease in the visible and NIR region of the spectrum. The PbS nanoparticles displayed very poor reflection of light throughout the UV-VIS-NIR region of the electromagnetic spectrum.

Direct band gap of the PbS nanoparticles sample was determined by plotting $(\alpha h\nu)^2$ versus $h\nu$ and then extrapolating the straight portion of the Tauc plots as shown in Figure 1d. The value of optical band gap was found to be 3.98eV for PbS nanoparticles dispersed in ethanol and 4.06eV for PbS nanoparticles dispersed in distilled water. This result agrees with several studies on PbS nanoparticles obtained in literatures [11] [9][10].

“It is reported that the band gap of a specific material does not only depend on its structure but the size also has a controlling factor. Once the particle reaches nano-meter size, quantum effects come into play and the effective band gap increases. Increasing bandgap energies of

PbS nanoparticles could be evidence of the quantum confinement effect due to decreasing size of structures”[15] [7].

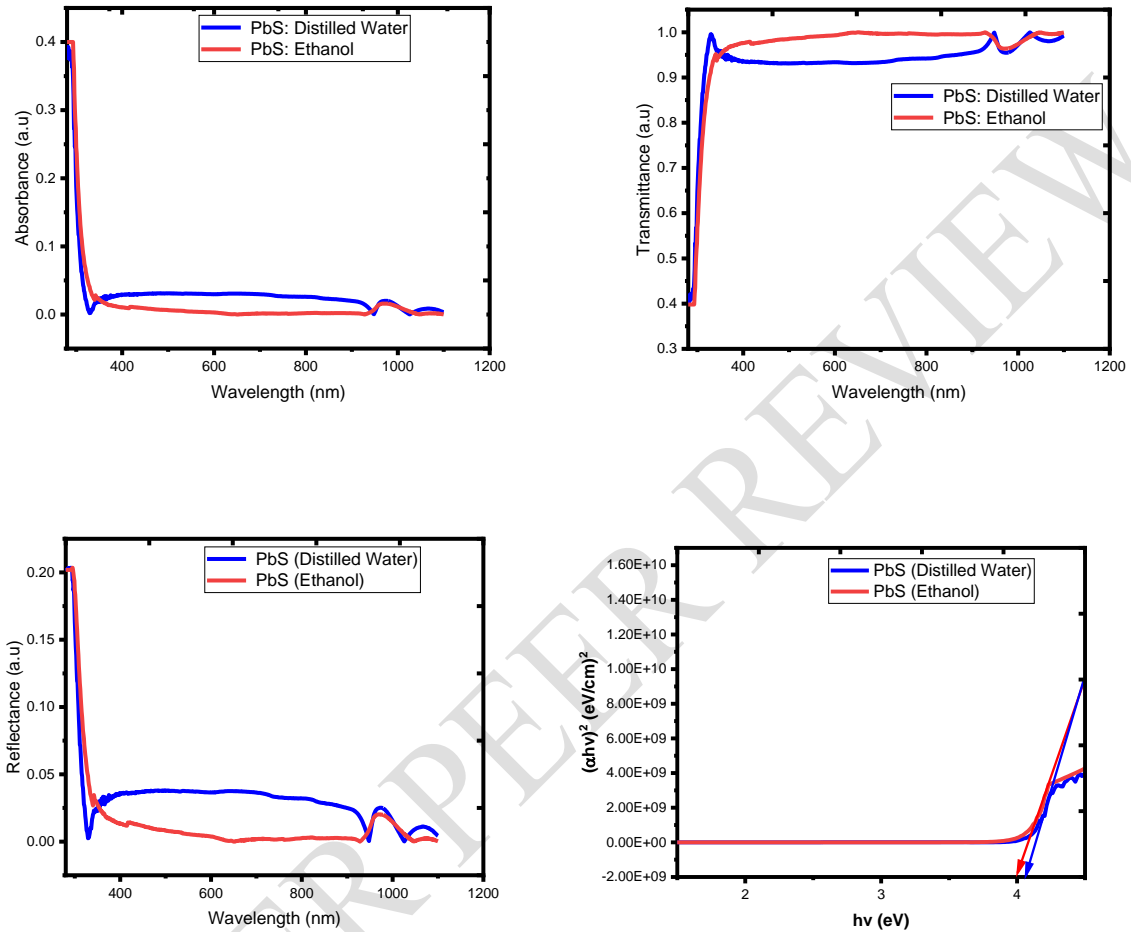


Figure 1(a) Absorbance spectra of PbS nanoparticles, (b) Transmittance spectra of PbS nanoparticles, (c) Reflectance spectra of PbS nanoparticles, (d) Optical energy bandgap plot of PbS nanoparticles

3.4 Surface morphological investigation of PbS nanoparticles

“The SEM characterization of PbS nanoparticles was done at University of Cape town, with Scanning Electron Microscope Carl Zeiss EVO 18 instrument. The topographical images obtained with non-conducting mode with different magnifications are shown in Figure 2. According to the SEM microstructural investigation, SEM images confirm the formation of cubic shaped nanoparticles”. [17] [22].

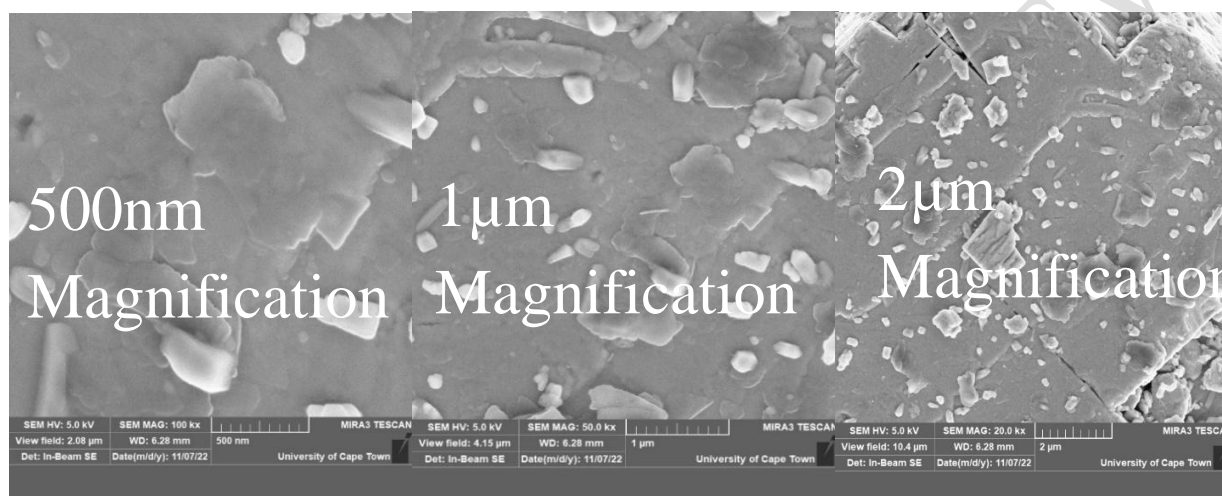


Figure 2: SEM micrographs of PbS nanoparticles

3.5 Elemental Composition of PbS Nanoparticles

Figure 3 shows the analysis of the elemental composition of PbS nanoparticles using Energy dispersive X-ray (EDX). The EDX revealed the compound composition of all the element its composed [12] [4]. The energy dispersive X-ray (EDX) analysis of PbS (Table 3) also revealed that the chemical components was predominantly of 54.36% Pb, followed by 36.47% C and 9.16% S.

Table 3: Atomic weight percentages of constituent elements in EDX spectra

PbS Nanoparticles	
Element	Atomic Weight (%)
Lead	54.36
Sulfur	9.16
Carbon	36.47

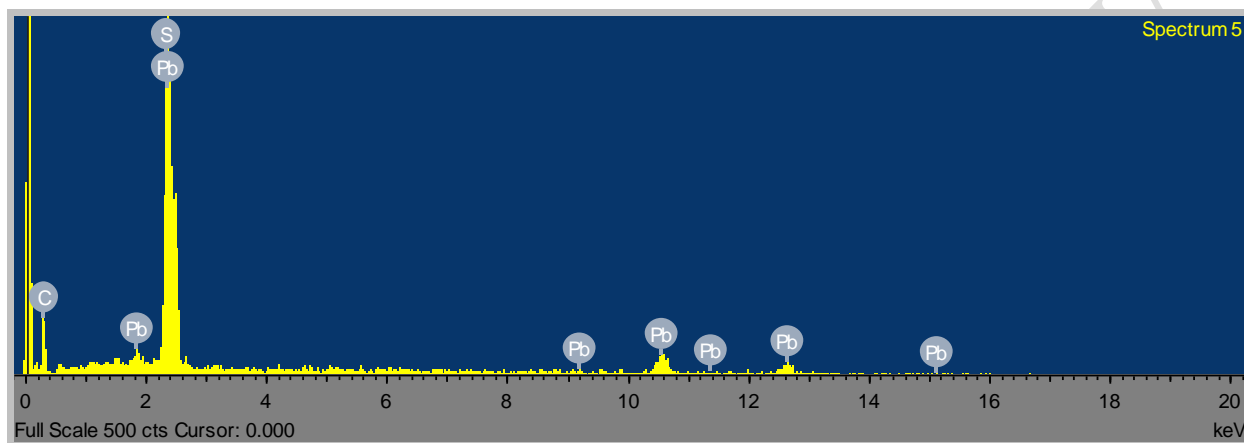


Figure 3: EDX spectrum of PbS nanoparticles

3.6 Structural analysis of PbS nanoparticles

Structural investigation of PbS nanoparticles was carried out using X-ray powder diffractometer (XRD) with a Cu-K α radiation source ($\lambda = 1.5406 \text{ \AA}$). Figure 4 shows the PbS nanoparticles XRD diffraction pattern. Distinct peaks of the PbS nanoparticles were observed at 21.65° , 23.11° , 23.77° , 28.70° , 32.78° and 47.04° corresponding to (111), (200), (210), (211), and (320) crystallographic planes. Some XRD peaks are left out without indexing because they might have been created by contaminants in the sample. The broadening of peaks in the XRD pattern indicates the nanocrystalline nature of the samples. [4] [2]. The average crystallite sizes were calculated using the Debye-Scherrer equation [18] [5] [24]. The average crystallite size of

PbS nanoparticles was found to be 51.05 nm.

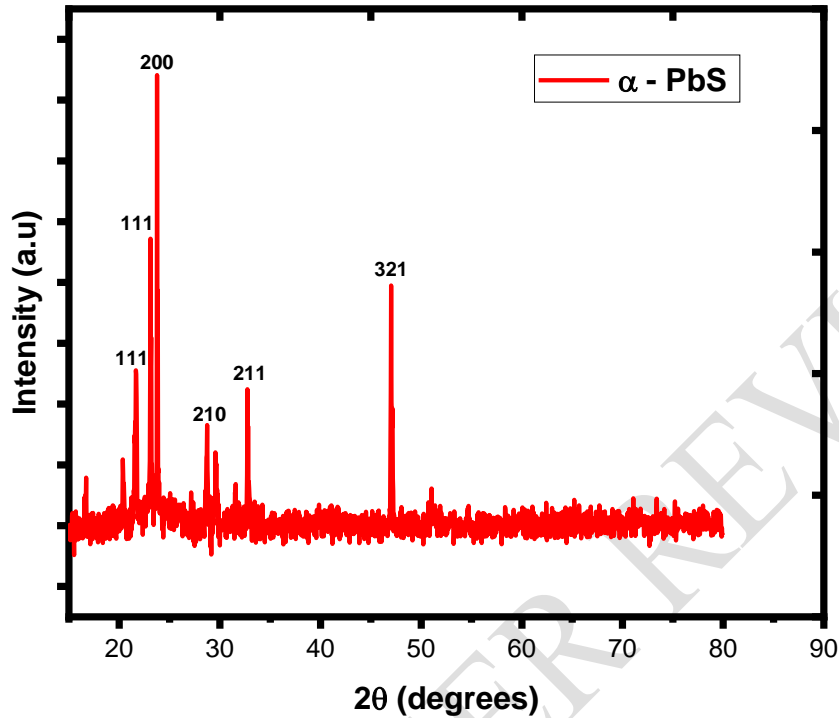


Figure 4: X-Ray Diffraction pattern for PbS nanoparticles

3.6 Electrical Properties

Using the four-point probe technique, the electrical (I-V) measurement PbS nanoparticles was determined. The nanoparticles were applied to a glass substrate using Dr blading method before the electrical investigation was performed. Figure 5 shows the average current and the related voltage. We noticed that the current passing through the film rises linearly as the electrode's voltage increases. This suggests that the film has a higher conductivity, which could assist in the production of solar cells with a higher frequency fabrication [21]. The average current and voltage of PbS thin film were found to be 3.85×10^{-8} A and 12.8×10^{-2} V. The resistivity (ρ) was estimated using the relation relation[6].

$$\rho = \frac{\pi}{\ln 2} \left(\frac{V}{I} \right) \times W \quad (1)$$

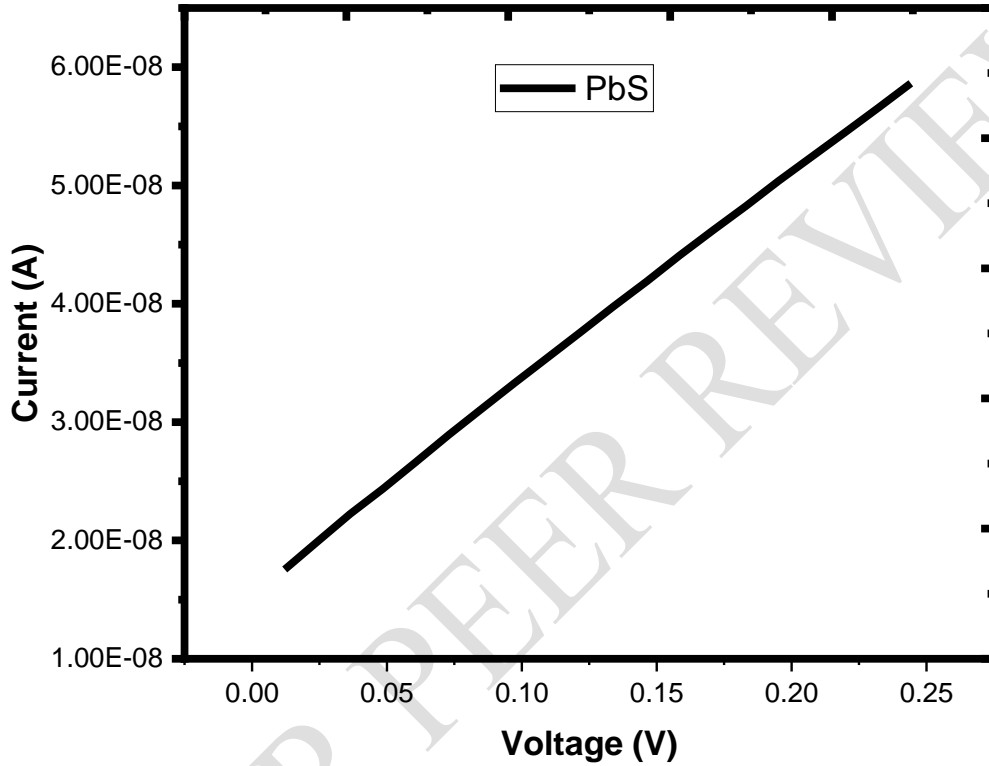


Figure 5: I-V characteristic of PbS nanoparticles

Where W is the film thickness, whose value 239.85 nm for PbS nanoparticles on the glass substrate. V and I are the average voltage and current of the film respectively. The reciprocal of the resistivity was taken as the conductivity (σ) of the film.

$$\sigma = \frac{1}{\rho} \quad (2)$$

from the values of resistivity (ρ) and thickness (W), the sheet resistance (R_s) can be determined as

$$R_s = \frac{\rho}{W} \quad (3)$$

The sheet resistance for PbS was found to be $1.51 \times 10^7 \Omega/\text{Sq.}$, the resistivity was calculated to be $3.61 \Omega.\text{cm}$ and the conductivity was also calculated to be $2.77 \times 10^{-1} (\Omega.\text{cm})^{-1}$. The electrical conductivity value falls within the magnitude of 10^{-13} to 10^2 reported for semiconducting thin films in literature [16], suggesting that the deposited film is conductive in nature. The observed high resistive value of the film indicates that it could find application as semiconducting sensors.

Conclusions

Lead sulphide (PbS) nanoparticles had been successfully processed utilizing a mechanical milling technique. The processed PbS nanoparticles were characterized using X-ray diffraction (XRD), atomic absorption spectroscopy (AAS), scanning electron microscopy (SEM) and UV-visible spectroscopy, energy dispersive analysis (EDAX), to study their structural, concentration of elements in the given sample, morphological, optical properties and elemental composition of the samples.

The PbS nanoparticles' XRD measurements reveal peaks at the crystal plane (111), (200), (210), (211) and (320). The average crystallite size of PbS nanoparticles was found to be 51.05 nm. The optical energy band gap was found to be 3.98 eV for PbS nanoparticles dispersed in ethanol and 4.06 eV for PbS nanoparticles dispersed in distilled water. The absorbance of PbS nanoparticles shows that the absorbance values were moderate in the UV region but dramatically decreased as they moved towards the visible and near-infrared regions. The PbS nanoparticles displayed very high transmittance and very poor reflection of light of throughout the UV-VIS-NIR region of the electromagnetic spectrum

PbS nanoparticles contain 54.36% Pb, 36.47% C and 9.16% S according to elemental analysis of their composition. The sheet resistance, resistivity, and conductivity were measured and found to be $1.51 \times 10^7 \Omega/\text{Sq.}$, $3.61 \Omega.\text{cm}$ and $2.77 \times 10^{-1} (\Omega.\text{cm})^{-1}$, respectively.

References

1. Chander, H. (2005). Development of nanophosphors—A review. *Materials Science and Engineering: R: Reports*, 49(5), 113-155
2. Chaudhary, M. D., Patel, J. C., & Chaudhari, J. M. (2016). Study of PbS nanoparticles synthesized by chemical route. *Int. J. Inno. Res. Mult. Field*, 2(12), 263-266.
3. Chongad, L. S., Sharma, A., Banerjee, M., & Jain, A. (2016, October). Synthesis of lead sulfide nanoparticles by chemical precipitation method. In *Journal of Physics: Conference Series* (Vol. 755, No. 1, p. 012032). IOP Publishing.
4. Dengo, N., Vittadini, A., Natile, M. M., & Gross, S. (2020). In-depth study of ZnS nanoparticle surface properties with a combined experimental and theoretical approach. *The Journal of Physical Chemistry C*, 124(14), 7777-7789.
5. Ebnalwaled, A. A., Essai, M. H., Hasaneen, B. M., & Mansour, H. E. (2017). Facile and surfactant-free hydrothermal synthesis of PbS nanoparticles: the role of hydrothermal reaction time. *Journal of Materials Science: Materials in Electronics*, 28(2), 1958-1965.
6. Emegha, J. O., Elete, E. D., Efe, F. O. O., & Adebisi, A. C. (2019). Optical and electrical properties of semiconducting ZnS thin film prepared by chemical bath deposition technique. *catalysis*, 3, 4.
7. Hamed, Z. H., Ahmed, K. E. A., & Elsheikh, H. A. (2021). Synthesis and characterization of ZnS nanoparticles by chemical precipitation method. *Aswan University Journal of Environmental Studies*, 2(2), 147-154.
8. Hassan, Z. W., Mohammed, M. S., & Jawad, M. F. (2023). Preparation and characterization of PbS nanoparticles by laser ablation technique. *Journal of Optics*, 1-6.
9. Himadri, D., Pranayee, D., & Kumar, S. K. (2018). Synthesis of pbs nanoparticles and its potential as a biosensor based on memristic properties. *Journal of Nanoscience and Technology*, 500-502.
10. Kumar, D., Agarwal, G., Tripathi, B., Vyas, D., & Kulshrestha, V. (2009). Characterization of PbS nanoparticles synthesized by chemical bath deposition. *Journal of Alloys and Compounds*, 484(1-2), 463-466.
11. Mamiyev, Z. Q., & Balayeva, N. O. (2015). Preparation and optical studies of PbS nanoparticles. *Optical Materials*, 46, 522-525.
12. Mishra, A. K., & Saha, S. (2022). Structural, electrical, and optoelectrical characterization of PbS nanoparticles. *JOURNAL OF OPTOELECTRONICS AND ADVANCED MATERIALS*, 24(5-6), 263-271.
13. Nabiyouni, G., Moghimi, E., Hedayati, K., & Jalajerdi, R. (2012). Room temperature synthesis of lead sulfide nanoparticles. *Main Group Metal Chemistry*, 35(5-6), 173-178.
14. Ndukwe, F., & Ekpunobi, A. (2023). Processing and Characterization of Limestone Nanoparticles. *American Journal of Physical Sciences*, 1(1), 63-70.
15. Nwauzor, J. N., Ekpunobi, A. J., & Babalola, A. D. (2023). Processing and Characterization of Iron Oxide Nanoparticle Produced by Ball Milling Technique. *Asian Journal of Physical and Chemical Sciences*, 11(1), 27-35.
16. Okafor, P. C., Ekpunobi, A. J., & Ekwo, P. A. (2014). Effect of manganese percentage doping on thickness and conductivity of zinc sulphidenanofilms prepared by electrodeposition method. *International Journal of Science and Research (IJSR)*, 4, 2275-2279.
17. Ologundudu, S. K., Ekpunobi, A. J., & Ikhioya, I. L. (2022). Synthesis and Characterization of ZnS Nanoparticles by Ball Milling Technique.

18. Onu, C. P., Ekpunobi, A. J., Okafor, C. E., & Ozobialu, L. A. (2023). Optical Properties of Monazite Nanoparticles Prepared Via Ball Milling. *Asian Journal of Research and Reviews in Physics*, 7(4), 17-29.
19. Saba, S., Bera, K & Jana, P.C. (2011). Growth time dependence of size of nanoparticles of ZnS, *International Journal of Soft Computing and Engineering (IJSCE)*. Vol. 1, Issue 5. pp 23.
20. Selim, H., Khalil, M. M. H., Al-Kotb, M. S., Kotkata, M. F., & Amer, H. H. (2013). Synthesis and structural characterization of ZnS quantum dots. *Journal of Radiation Research and Applied Sciences*, 6(1), 89-103.
21. Thirumavalavan, S., Mani, K., & Sagadevan, S. (2015). Studies on structural, surface morphology and optical properties of zinc sulphide (ZnS) thin films prepared by chemical bath deposition. *International Journal of Physical Sciences*, 10(6), 204-209.
22. Tshemese, Z., Khan, M. D., Mlowe, S., & Revaprasadu, N. (2018). Synthesis and characterization of PbS nanoparticles in an ionic liquid using single and dual source precursors. *Materials Science and Engineering: B*, 227, 116-121.
23. Vikesland, P. J., & Wigginton, K. R. (2010). Nanomaterial enabled biosensors for pathogen monitoring-a review. *Environmental science & technology*, 44(10), 3656-3669
24. Yimin, D., Jiaqi, Z., Danyang, L., Lanli, N., Liling, Z., Yi, Z., & Xiaohong, Z. (2018). Preparation of Congo red functionalized Fe₃O₄@ SiO₂ nanoparticle and its application for the removal of methylene blue. *Colloids and Surfaces A: Physicochemical and Engineering Aspects*, 550, 90-98.
25. Zaragoza-Palacios, B. G., Torres-Duarte, A. R., & Castillo, S. J. (2021). Synthesis and characterization of nanoparticles and thin films of PbS by a high-performance procedure using CBD. *Journal of Materials Science: Materials in Electronics*, 32, 22205-22213.
26. Ologundudu SK, Ekpunobi AJ, Ikhioya IL. Synthesis and Characterization of ZnS Nanoparticles by Ball Milling Technique. *SSRG International Journal of Material Science and Engineering* Volume 8 Issue 3, 6-13, Sep-Dec 2022